J|A|C|S
ARTICLES
Published on Web 05/24/2002

Metal Ion-Induced Site-Selective RNA Hydrolysis by Use of Acridine-Bearing Oligonucleotide as Cofactor

Akinori Kuzuya, Ryo Mizoguchi, Fumi Morisawa, Kenzo Machida, and Makoto Komiyama*

Contribution from the Research Center for Advanced Science and Technology, The University of Tokyo, 4-6-1 Komaba, Meguro, Tokyo 153-8904, Japan

Received January 21, 2002

Abstract: New types of noncovalent ribozyme-mimics for site-selective RNA scission are prepared by combining metal ions with oligonucleotides bearing an acridine. Lanthanide(III) ions and various divalent metal ions (Zn(II), Mn(II), Cu(II), Ni(II), Co(II), Mg(II), and Ca(II)) are employed without being bound to any sequence-recognizing moiety. The modified oligonucleotide forms a heteroduplex with the substrate RNA, and selectively activates the phosphodiester linkages in front of the acridine. As a result, these linkages are preferentially hydrolyzed over the others, even though the metal ions are not fixed anywhere. The scission is efficient under physiological conditions, irrespective of the sequence at the target site. Site-selective RNA scission is also successful with the combination of an oligonucleotide bearing an acridine at its terminus, another unmodified oligonucleotide, and the metal ion. In a proposed mechanism, the acridine pushes the unpaired ribonucleotide out of the heteroduplex and changes the conformation of RNA at the target site for the sequence-selective activation.

Introduction

Site-selective scission of RNA has been attracting the interest of chemists and biochemists as it is indispensable for molecular biology and therapy in the future.[1] RNA enzymes (ribozymes) discovered by Cech et al. have been widely used for this purpose.[2] Furthermore, totally man-made ribozyme-mimics have been prepared by attaching inorganic or organic scissors to oligonucleotides which bind the substrate RNA near the target site.[3−5] Their site-selectivity originates primarily from a favorable activation-entropy term for the hydrolysis of target phosphodiester linkage.

Another strategy for the preparation of site-selective artificial ribonucleases takes advantage of the difference in reactivity between the target site and the others. For example, bulge-structures[6] and gap-structures[7] were intentionally formed in RNA by using appropriate oligonucleotides, and these composites were treated with molecular scissors. The bulge-sites and unpaired-sites were preferentially hydrolyzed, mainly because the double-stranded portion is less reactive than is the single-stranded portion. These findings have strongly indicated that still more efficient and clear-cut RNA scission should be accomplished if one can somehow activate the target phosphodiester linkage.[8,9] Here we show that site-selective RNA activation is successfully achieved by oligonucleotides bearing an acridine. The target sites are efficiently hydrolyzed by lanthanide ions and various divalent ions (e.g., Zn(II) and Mn(II)), even though they are not bound to any sequence-recognizing moiety. The factors required for the site-selective scission are precisely pinned down. Furthermore, dependencies of scission efficiency on the kind of metal ion, the sequence of target site, and the mismatches at the scission site are clarified. The catalytic mechanism is proposed in terms of these results and spectroscopic evidence.

Results

In the present study, two types of RNA activators are used for site-selective RNA scission (see Figure 1). The type-I activators are modified oligonucleotides that bear an acridine derivative in the middle (e.g., DNA_{F1}-Acr, DNA_{F2}-Acr, and

* Corresponding author. E-mail: komiyama@mkomi.rcast.u-tokyo.ac.jp.

(1) A recent publication on RNA scission: *Methods Enzymol.* **2001**, *341*, 1−734.

(2) (a) Cech, T. R. *Science* **1987**, *236*, 1532−1539. (b) Breaker, R. R. *Chem. Rev.* **1997**, *97*, 371−390.

(3) Reviews: (a) Komiyama, M.; Sumaoka, J.; Kuzuya, A.; Yamamoto, Y. *Methods Enzymol.* **2001**, *341*, 455−468. (b) Trawick, B. N.; Daniher, A. T.; Bashkin, J. K. *Chem. Rev.* **1998**, *98*, 939−960.

(4) (a) Matsumura, K.; Endo, M.; Komiyama, M. *J. Chem. Soc., Chem. Commun.* **1994**, 2019−2020. (b) Hall, J.; Hüsken, D.; Häner, R. *Nucleic Acids Res.* **1996**, *24*, 3522−3526. (c) Magda, D.; Wright, M.; Crofts, S.; Lin, A.; Sessler, J. L. *J. Am. Chem. Soc.* **1997**, *119*, 6947−6948. (d) Inoue, H.; Furukawa, T.; Shimizu, M.; Tamura, T.; Matsui, M.; Ohtsuka, E. *Chem. Commun.* **1999**, 45−46. (e) Baker, B. F.; Lot, S. S.; Kringel, J.; Cheng-Flournoy, S.; Villiet, P.; Sasmor, H. M.; Siwkowski, A. M.; Chappell, L. L.; Morrow, J. R. *Nucleic Acids Res.* **1999**, *27*, 1547−1551. (f) Putnam, W. C.; Daniher, A. T.; Trawick, B. N.; Bashkin, J. K. *Nucleic Acids Res.* **2001**, *29*, 2199−2204.

(5) (a) Hovinen, J.; Guzaev, A.; Azhayeva, E.; Azhayev, A.; Lönnberg, H. *J. Org. Chem.* **1995**, *60*, 2205−2209. (b) Reynolds, M. A.; Beck, T. A.; Say, P. B.; Schwartz, D. A.; Dwyer, B. P.; Daily, W. J.; Vaghefi, M. M.; Metzler, M. D.; Klem, R. E.; Arnold, L. J., Jr. *Nucleic Acids Res.* **1996**, *24*, 760−765. (c) Endo, M.; Azuma, Y.; Saga, Y.; Kuzuya, A.; Kawai, G.; Komiyama, M. *J. Org. Chem.* **1997**, *62*, 846−852. (d) Beloglazova, N. G.; Sil'nikov, V. N.; Zenkova, M. A.; Vlassov, V. V. *FEBS Lett.* **2000**, *481*, 277−280.

(6) (a) Hüsken, D.; Goodall, G.; Blommers, M. J. J.; Jahnke, W.; Hall, J.; Häner, R.; Moser, H. E. *Biochemistry* **1996**, *35*, 16591−16600. (b) Kaukinen, U.; Bielecki, L.; Mikkola, S.; Adamiak, R. W.; Lönnberg, H. *J. Chem. Soc., Perkin Trans. 2* **2001**, 1024−1031.

(7) Kuzuya, A.; Akai, M.; Komiyama, M. *Chem. Lett.* **1999**, 1035−1036.

(8) Kuzuya, A.; Komiyama, M. *Chem. Commun.* **2000**, 2019−2020.

(9) Kuzuya, A.; Komiyama, M. *Chem. Lett.* **2000**, 1378−1379.

10.1021/ja025653p CCC: $22.00

Substrate

RNA_1 5' UGA GAC GAU GAC UGG AUC UGG CAC UAC GAC ACU UGG 3'

Type I RNA-activators

DNA_{F1}-Acr 3' ACT CTG CTA CTG ACC TAG **X**CC GTG ATG CTG TGA ACC 5'

DNA_{F2}-Acr 3' ACT CTG CTA CTG ACC TA**X** ACC GTG ATG CTG TGA ACC 5'

DNA_{F3}-Acr 3' ACT CTG CTA CTG ACC TAG A**X**C GTG ATG CTG TGA ACC 5'

DNA_{F1} 3' ACT CTG CTA CTG ACC TAG – CC GTG ATG CTG TGA ACC 5'

DNA_{F1}-S 3' ACT CTG CTA CTG ACC TAG **S**CC GTG ATG CTG TGA ACC 5'

X = 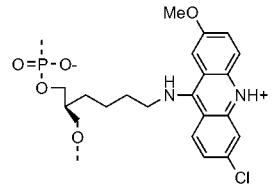

S = 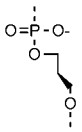

Type II RNA-activators

3' ACC GTG ATG CTG TGA ACC 5' DNA_{R2}

DNA_{L1}-Acr 3' ACT CTG CTA CTG ACC TAG **Y** 5' 3' CC GTG ATG CTG TGA ACC 5' DNA_{R1}

3' C GTG ATG CTG TGA ACC 5' DNA_{R3}

DNA_{L1} 3' ACT CTG CTA CTG ACC TAG 5' 3' **Y**CC GTG ATG CTG TGA ACC 5' Acr-DNA_{R1}

Y = 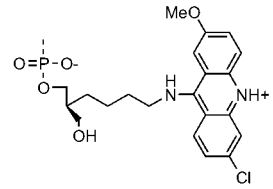

Figure 1. Structures of RNA substrate and its activators.

DNA_{F3}-Acr). Unless otherwise noted, 9-amino-6-chloro-2-methoxyacridine is used.[10] The type-II activators are composed of two oligonucleotides, one of which has an acridine at its terminus (DNA_{L1}-Acr/DNA_{R1} and DNA_{L1}/Acr-DNA_{R1} combinations). None of the metal ions used in this study alters the UV−vis absorption spectra of these modified oligonucleotides in aqueous solutions. Complex formation between the acridine and the metal ions is unlikely.[11]

Site-Selective RNA Scission by Lanthanide(III) Ions. In the heteroduplex between substrate RNA_1 and DNA_{F1}-Acr as type-I activator, the U19 of RNA_1 faces the acridine and only this ribonucleotide remains unpaired.[12] When $LaCl_3$, $EuCl_3$, and $LuCl_3$ are added to this system, site-selective RNA scission is successfully accomplished (lanes 3, 6, and 9 in Figure 2). The scission occurs overwhelmingly at the 5′-side of the unpaired ribonucleotide U19 or its 3′-side (Figure 3a). After 2 h at pH 8.0 and 37 °C, the total conversions of the selective scission are 23, 19, and 17% for La(III), Eu(III), and Lu(III), respectively ($[LnCl_3]_0 = 100\ \mu M$). The site-selective scission is also effective at pH 7.0, and the conversion of RNA cleavage by Lu(III) is 29%.[13] With the use of DNA_{F1}-S, which has no acridine, however, the scission is much slower (lanes 2, 5, and 8 in Figure 2). The ratio of the scission rate by DNA_{F1}-Acr to the rate by DNA_{F1}-S is shown in Figure 4. Regardless of the kind of lanthanide ion and the scission site (either the 5′-side of U19 or its 3′-side), this ratio (an index for the magnitude of acceleration by the acridine) is far greater than 1. For example, the scission at the 5′-side by the DNA_{F1}-Acr/Lu(III) system is 14 times as fast as that by the DNA_{F1}-S/Lu(III) system. Apparently, the target phosphodiester linkages are selectively and efficiently activated by the acridine in DNA_{F1}-Acr. In contrast, the other phosphodiester linkages are deactivated when the heteroduplex is formed. Because of the cooperation of these two factors, the discrimination of the target linkage from the others is sufficiently clear-cut. In the absence of oligonucleotide, all the lanthanide ions cut the RNA almost randomly (lanes 1, 4, and 7).

(10) Use of 9-amino-6-chloro-2-methoxyacridine as intercalator was previously reported: (a) Nelson, P. S.; Kent, M.; Muthini, S. *Nucleic Acids Res.* **1992**, *20*, 6253−6259. (b) François, J. C.; Hélène, C. *Bioconj. Chem.* **1999**, *10*, 439−446.

(11) Note that the 9-amino-6-chloro-2-methoxyacridine exists mostly in its protonated form under the conditions employed ($pK_a = 8.5$: Albert, A. In *The acridines*, 2nd ed.; Edward Arnold Publishers Ltd.: London, UK, 1966; pp 434−467).

(12) The melting temperature (T_m) of RNA_1/DNA_{F1}-Acr heteroduplex is higher than 80 °C, and thus this duplex is almost completely formed under the reaction conditions.

(13) The scission rate linearly increases with the increase in [Lu(III)].

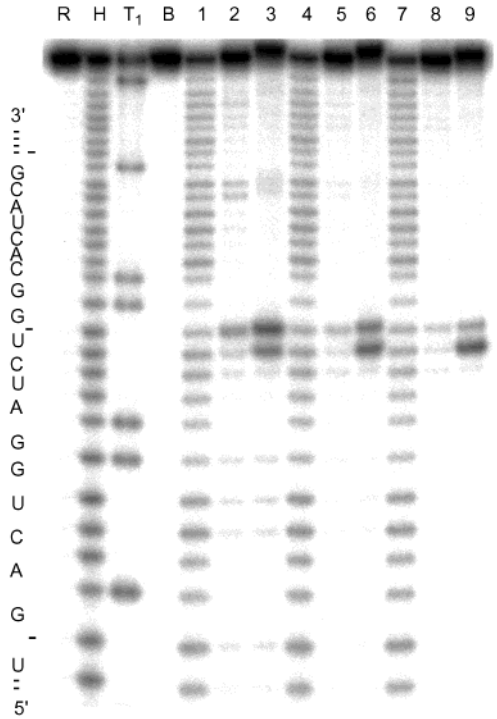

Figure 2. Site-selective RNA scission by combinations of type-I activator and lanthanide(III) ion. Lane 1, La(III) only; lane 2, DNA_{F1}-S/La(III); lane 3, DNA_{F1}-Acr/La(III); lane 4, Eu(III) only; lane 5, DNA_{F1}-S/Eu(III); lane 6, DNA_{F1}-Acr/Eu(III); lane 7, Lu(III) only; lane 8, DNA_{F1}-S/Lu(III); lane 9, DNA_{F1}-Acr/Lu(III). At pH 8.0 and 37 °C for 2 h; $[RNA_1]_0 = 1$, $[DNA_{F1}\text{-S}]_0 = [DNA_{F1}\text{-Acr}]_0 = 10$, and $[LnCl_3]_0 = 100\ \mu M$; $[NaCl]_0 = 200$ mM. R, RNA_1 only; H, alkaline hydrolysis; T_1, RNase T_1 digestion; B, control reaction in buffer solution.

Whether the scission occurs dominantly at the 5′-side of the unpaired ribonucleotide or its 3′-side is strongly dependent on the kind of lanthanide ion used in the reaction (Figure 5a). As the atomic number in the lanthanide series increases, the scission at the 5′-side is gradually promoted (the filled bars). On the other hand, the scission at the 3′-side is suppressed (the shaded bars). As a result, the 5′/3′ ratio for each of the lanthanide ions between Pr and Ho monotonically increases with increasing atomic number, and attains a plateau there (Figure 5b). Heavy rare-earth metal ions preferentially hydrolyze the 5′-side, whereas light rare-earth metals choose the 3′-side. Thus, the scission site can be modulated by the use of the appropriate lanthanide ion.

Effect of the Sequence at the Target Site on Site-Selective Scission. By changing the modified oligonucleotide and moving the position of acridine in the RNA/DNA heteroduplex, the site of selective scission can be freely altered. A typical example with Lu(III) is presented in Figure 6. When C18 in RNA_1 is kept unpaired by using DNA_{F2}-Acr, the linkage in the 5′-side of C18 is preferentially hydrolyzed (lane 2). Making U19 unpaired by DNA_{F1}-Acr leads to the scission at its 5′-side, as described above (lane 3). With G20 unpaired (by DNA_{F3}-Acr), the major scission site is also its 5′-side (lane 4). The rates of scissions are not significantly different from each other. The present selective scission is successful irrespective of the sequence at the scission site. This conclusion has been further confirmed by systematic studies with various RNA substrates (see Supporting Information, Table 1). The site-selective scission by the other lanthanide ions (and also by various divalent metal ions) is also less dependent on the sequence at the target site.

Essential Factors Required for the Site-Selective RNA Scission. The DNA_{L1}-Acr/DNA_{R1} combination (the type-II activator; Figure 3b) is also effective for the site-selective scission. By comparing lane 3 in Figure 7 with lane 2 for the DNA_{L1}/DNA_{R1} combination, the essential role of the acridine in the activation of the target site is evident. Site-selective RNA scission is also successful by combining an unmodified oligonucleotide DNA_{L1} with another modified oligonucleotide Acr-DNA_{R1}, which bears an acridine at the 3′-end (lane 4). The scission efficiency is almost the same as that by the DNA_{L1}-Acr/DNA_{R1}/Lu(III) system. Thus, an acridine residue can be attached to either of these two oligonucleotides. When both of the oligonucleotides have an acridine residue at the terminus (the combination of DNA_{L1}-Acr and Acr-DNA_{R1}), however, the scission is inefficient (lane 5).

For these site-selective scissions, an acridine is introduced to the oligonucleotides in place of a nucleotide in front of the target site (thus, one ribonucleotide in the RNA is unpaired). Site-selective scission is also successful when two ribonucleotides are made unpaired by combining DNA_{R3} with DNA_{L1}-Acr (lane 4 in Figure 8). However, virtually no scission occurs when the DNA_{L1}-Acr/DNA_{R2} combination is used and all the ribonucleotides in RNA_1 form base pairs (lane 2). One or two ribonucleotides must remain unpaired for the selective scission. In lanes 5 and 6 in this figure, only one of the two oligonucleotides is used and many consecutive ribonucleotides are kept

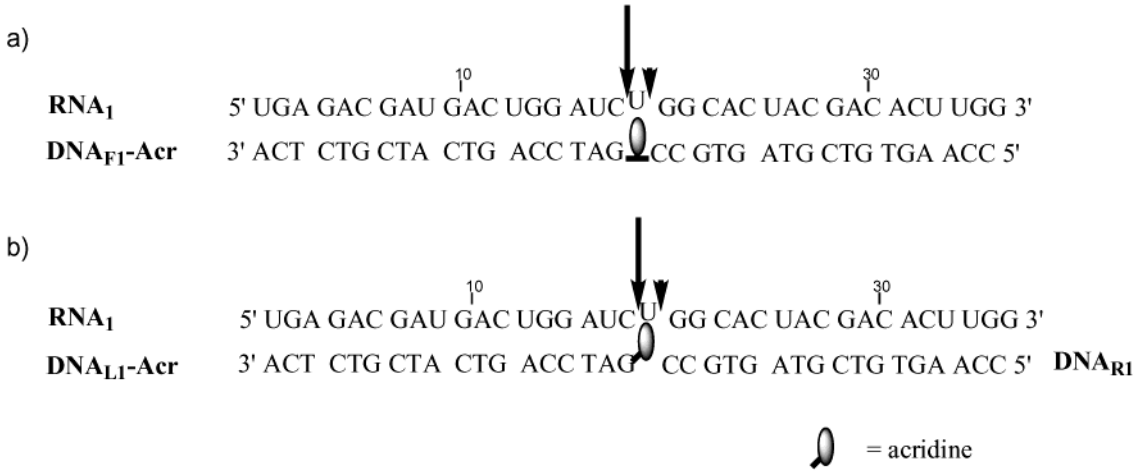

Figure 3. Site-selective scission by (a) the DNA_{F1}-Acr/Lu(III) system and (b) the DNA_{L1}-Acr/DNA_{R1}/Lu(III) system.

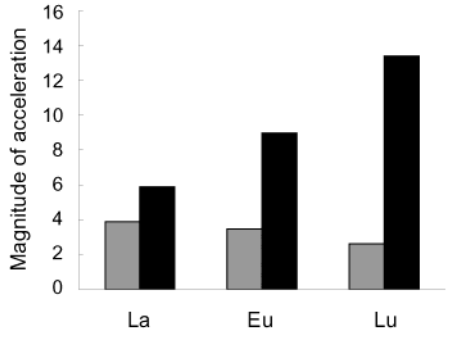

Figure 4. The ratio of the scission rate by DNA_{F1}-Acr to that by DNA_{F1}-S in the site-selective RNA scission (determined by using the results in Figure 2). Shaded bars are for the scission at the 3′-side of unpaired U19, and filled bars are for the 5′-side scission.

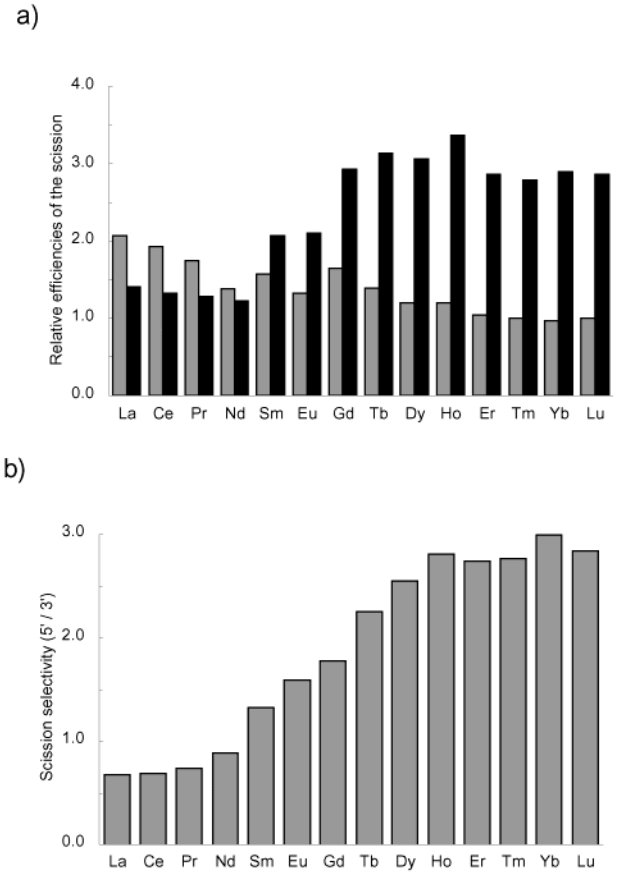

Figure 5. Relative efficiencies of the site-selective scission by the combinations of DNA_{F1}-Acr and various lanthanide ions (a). Shaded bars are for the 3′-side scission, and filled bars are for the 5′-side scission. The efficiency for the 3′-side scission by Lu(III) is taken as unity. In part b, the ratio of the 5′-side scission to the 3′-side scission for each lanthanide(III) ion is presented. The reaction conditions are described in the caption of Figure 2.

unpaired. Here, RNA is cleaved randomly throughout the single-stranded portion. Note that DNA_{L1}-Acr never accelerates the scission at U19 in the absence of DNA_{R1} (compare lanes 5 with 7).

Significantly, mismatches near the scission-site cause critical damage to the site-selective scission. When both of the ribonucleotides neighboring the target ribonucleotide (U19 in RNA_1) are mismatched (e.g., T in front of C18 and G in front of G20), the site-selective scission is completely gone (data not shown). It is noteworthy that the RNA is only marginally

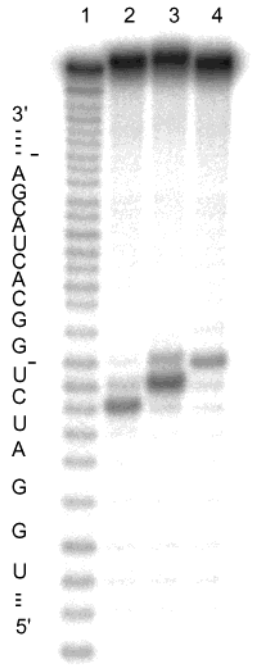

Figure 6. Effect of the sequence of target site on the site-selective RNA scission. Lane 1, Lu(III) only; lane 2, DNA_{F2}-Acr/Lu(III); lane 3, DNA_{F1}-Acr/Lu(III); lane 4, DNA_{F3}-Acr/Lu(III). At pH 8.0 and 37 °C for 2 h; $[RNA_1]_0 = 1$, [each modified oligonucleotide]$_0 = 10$, and $[LuCl_3]_0 = 100$ μM; $[NaCl]_0 = 200$ mM.

hydrolyzed when a one-base bulge structure is formed at U19 in RNA_1 by using the unmodified oligonucleotide DNA_{F1} (data not shown). This oligonucleotide is complementary with RNA_1 except for the lack of the counterpart of U19, but has no acridine. The RNA is not sufficiently activated by this simple bulge strategy. In contrast with the remarkable effects by the acridine-bearing oligonucleotides for the site-selective RNA scission, neither fluorescein- nor tetramethylrhodamine-bearing oligonucleotide was active.

Site-Selective RNA Scission by Zn(II), Mn(II), and Other Divalent Metal Ions. In the presence of $Zn(NO_3)_2$ and DNA_{F1}-Acr, RNA_1 is selectively and efficiently hydrolyzed at U19 under physiological conditions (lane 3 in Figure 9). The dominant scission site is the 5′-side of U19 (5′/3′ ratio = 6), which is identical with the scission site by heavy rare-earth metal ions. The conversion of the major scission by 1 mM Zn(II) after 16 h is 40% (more than 80% of the RNA is hydrolyzed in 48 h). The type-II activator (the DNA_{L1}-Acr/DNA_{R1} combination) is also effective. On the other hand, either DNA_{F1}-S or the DNA_{L1}/DNA_{R1} combination is poor at the RNA activation (see Supporting Information, Figure 1). The acridine group is absolutely necessary for this efficient site-selective scission.[14]

For the site-selective scission, Mn(II) is also effective. In contrast with the 5′-preference by Zn(II), the 3′-side of the unpaired ribonucleotide is more promptly hydrolyzed by Mn(II) (the 3′/5′ ratio is 4: lane 5 in Figure 9). As depicted in Figure 2 in the Supporting Information, Cu(II), Ni(II), and Co(II) ions are also active, but Fe(II) ion is virtually inactive. When Mg(II) is combined with DNA_{F1}-Acr, the linkage in the 3′-side of unpaired U19 is selectively hydrolyzed (Supporting Information, Figure 3). The conversion by 320 mM Mg(II) at 37 °C

(14) The scission by the DNA_{F1}-Acr/Zn(II) system is 10 times as fast as that by the DNA_{L1}/DNA_{R1}/Zn(II) system.

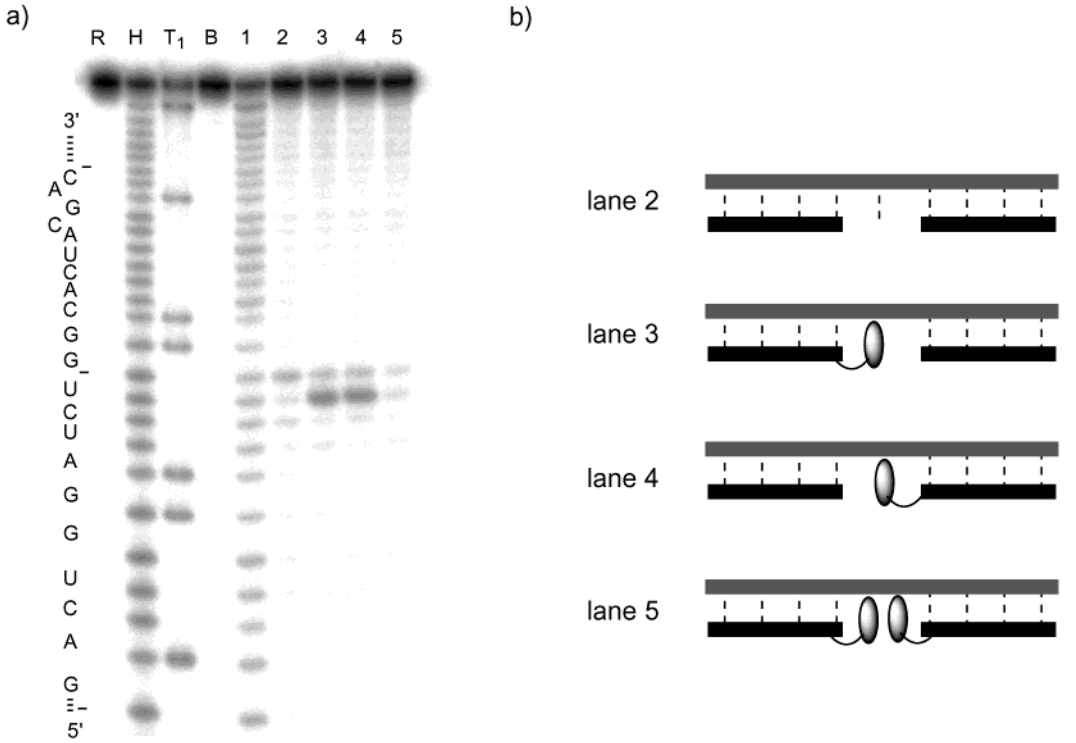

Figure 7. Site-selective RNA scission by various combinations of type-II activator and Lu(III). (a) PAGE patterns of the scission. Lane 1, Lu(III) only; lane 2, DNA_{L1}/DNA_{R1}/Lu(III); lane 3, DNA_{L1}-Acr/DNA_{R1}/Lu(III); lane 4, DNA_{L1}/Acr-DNA_{R1}/Lu(III); lane 5, DNA_{L1}-Acr/Acr-DNA_{R1}/Lu(III). At pH 8.0 and 37 °C for 2 h; $[RNA_1]_0 = 1$, [each modified or unmodified oligonucleotide]$_0 = 10$, and $[LuCl_3]_0 = 100$ μM; $[NaCl]_0 = 200$ mM. R−B are as described in the caption of Figure 2. (b) Schematic representations of the combinations used in part a.

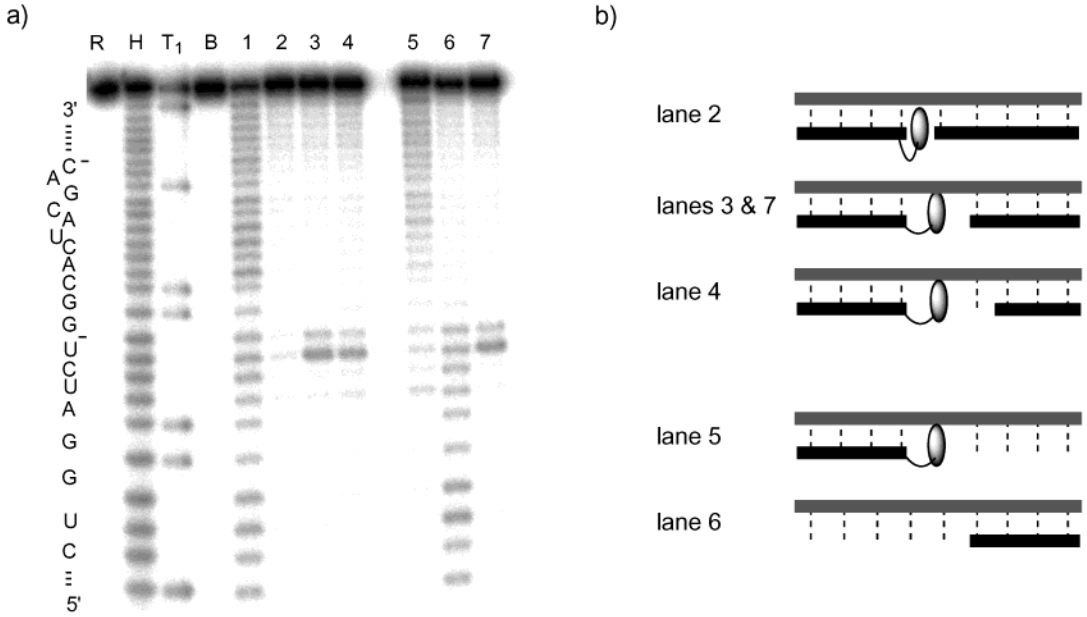

Figure 8. Effect of the number of unpaired ribonucleotides on the site-selective RNA scission by the combinations of type-II activator and Lu(III). (a) PAGE patterns of the scission. Lane 1, Lu(III) only; lane 2, DNA_{L1}-Acr/DNA_{R2}/Lu(III) ($n = 0$); lane 3, DNA_{L1}-Acr/DNA_{R1}/Lu(III) ($n = 1$); lane 4, DNA_{L1}-Acr/DNA_{R3}/Lu(III) ($n = 2$); lane 5, DNA_{L1}-Acr/Lu(III); lane 6, DNA_{R1}/Lu(III); lane 7, the same as in lane 3. At pH 8.0 and 37 °C for 2 h; $[RNA_1]_0 = 1$, [each modified or unmodified oligonucleotide]$_0 = 10$ and $[LuCl_3]_0 = 100$ μM; $[NaCl]_0 = 200$ mM. R−B are as described in the caption of Figure 2. (b) Schematic representations of the combinations used in part a.

and pH 8.0 after 16 h is 13%. The RNA scission by Ca(II) ion occurs also at the 3′-side of U19. As expected, Na(I) and K(I) ions showed no measurable activity.

Evidence for the Hydrolytic Scission. When the ribonucleotide C18 in RNA_1 is replaced by 2′-*O*-methylcytidine and this substrate is treated with the DNA_{F1}-Acr/Lu(III) system, the scission at the 3′-side of C18 (the 5′-side of U19) completely disappears (Supporting Information, Figure 4: note that this is the major scission-site for the parent RNA). The scission at the 3′-side of U19 is not much affected by this substitution. Similar replacement of U19 by 2′-*O*-methyluridine inhibits the scission at the 3′-side of U19. It is conclusive that the present site-selective RNA scission proceeds via intramolecular nucleophilic attack of the 2′-OH as does conventional RNA hydrolysis, and

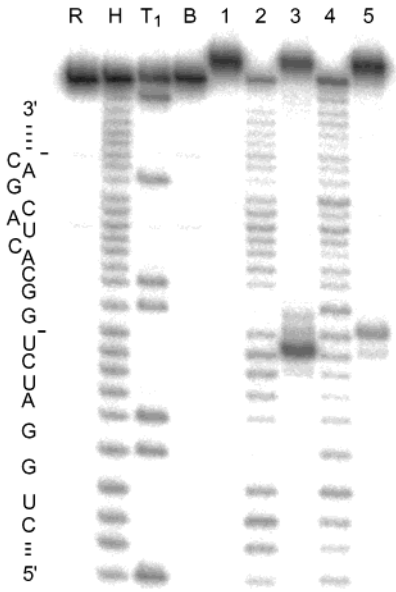

Figure 9. Site-selective scissions by Zn(II) and Mn(II). Lane 1, DNA_{F1}-Acr only; lane 2, Zn(II) only; lane 3, DNA_{F1}-Acr/Zn(II); lane 4, Mn(II) only; lane 5, DNA_{F1}-Acr/Mn(II). At pH 8.0 and 37 °C for 16 h; $[RNA_1]_0 = 1$ and $[DNA_{F1}\text{-Acr}]_0 = 10\ \mu M$; [metal nitrate]$_0$ = 1 mM; $[NaCl]_0 = 200$ mM. R−B are as described in the caption of Figure 2.

that the scissions at the 3′-side and the 5′-side proceed independently. According to MALDI TOF mass analyses, the present scission generates both 3′-(or 2′-)monophosphate termini and 5′-OH termini (see Supporting Information, Figure 5).[15]

Effect of the Substituents of Acridine on the RNA-Hydrolyzing Activity. To shed light on the reaction mechanism, various acridines with different substituents were conjugated to the 5′-end of DNA_{L1},[16] and used with DNA_{R1} as the Type-II activators (see Figure 10b: metal ion = Lu(III)). Under the reaction conditions, these acridines exist mostly in protonated form as does the one used hitherto (9-amino-6-chloro-2-methoxyacridine).[11] In Figure 10a, the logarithm of the pseudo-first-order rate constant of the scission at the 5′-side of U19 is plotted as a function of the pK_a value of acridine. As the pK_a decreases, the RNA-hydrolyzing activity monotonically increases. The slope is ca. −0.5. This linear correlation suggests that acid catalysis by the acridine participates in the scission. Consistently, 9-acridinecarboxamide, which has a smaller pK_a and exists mostly as neutral species in the reaction mixtures,[17] scarcely activates RNA even when it is attached to the oligonucleotides.[18]

Spectroscopic Analyses on the Complexes in the Reaction Mixtures. In the DNA_{L1}-Acr/DNA_{R1}/RNA_1 ternary system, the UV−Vis absorption band of the acridine in the 370−470 nm region shows a small but clear-cut hypochromicity (Figure 11a). The fluorescence from the acridine is notably quenched (Figure 11b). It is indicated that, in the ternary complex, the acridine ring is sandwiched between two base pairs and the adjacent two GC pairs quench the fluorescence (see Figure 3b).[19] Consistently, both the hypochromicity and the quenching are smaller in the binary DNA_{L1}-Acr/RNA_1 complex. Note that the second oligonucleotide DNA_{R1} is absolutely necessary for the site-selective RNA activation (lane 5 in Figure 8). The CD spectrum of the ternary complex is the one for a typical A-form duplex. The acridine of DNA_{L1}-Acr never induces a drastic change to the whole structure of the RNA/DNA heteroduplex.

Discussion

Characteristics of the Present Noncovalent Systems for Site-Selective RNA Scission. The present site-selective scissions are based on the activation of the target phosphodiester linkages by noncovalent interactions. The DNA_{F1}-Acr/Lu(III) system hydrolyzes about half of the substrate RNA at the target site within a half-day under physiological conditions. This scission is about 2 times as fast as the site-selective RNA scission by the covalent conjugate of Lu(III) complex and oligonucleotide,[4a] although it is an intermolecular reaction and does not accompany so-called "proximity effect". Apparently, the unfavorable activation-entropy term is sufficiently compensated by the site-selective activation of the target site. Furthermore, the metal ions are free from complex formation with strong ligands and satisfactorily retain their intrinsic catalytic activity.

Accordingly, even poor molecular scissors can be used in the present noncovalent systems. For example, Zn(II) ion and its complexes are usually inappropriate for the catalytic centers of covalent artificial enzymes.[20] In the present noncovalent systems, however, the Zn(II) ion is sufficiently active for RNA hydrolysis (its activity is only 10-fold smaller than that of the Lu(III) ion, which is one of the most active catalysts ever reported). As a molecular scissor, Mn(II) is also available. Even the Mg(II) ion shows a reasonable activity. A strong potential of the present noncovalent systems for variety of applications is indicated.

Site of Selective RNA Scission. It is important that the site-selective scission efficiently occurs irrespective of the sequence at the target site (Figure 6). Thus, there is no limitation in the choice of RNA substrate and the selective-scission site. With conventional ribozymes, however, the scission requires specific sequences. For example, the scission by hammerhead ribozyme is notable only at the sequence NUX (N = A, G, C, or T, and X = A, C, or T),[21] while hairpin ribozymes choose the GUC sequence.[22] If the corresponding sequence cannot be found near the target site in practical applications, specially designed ribozymes are necessary.[23]

The RNA scission occurs at the 5′-side or the 3′-side of the unpaired ribonucleotide (in front of the acridine). Which linkage

(15) The 2′,3′-cyclic monophosphates formed during the reactions were rapidly hydrolyzed and not much accumulated. Lanthanide ions are very active for the hydrolysis of these cyclic phosphates: Matsumura, K.; Komiyama, M. *J. Biochem.* **1997**, *122*, 387−394.
(16) For synthetic convenience, a simple alkyl chain was used as the linker for these acridine-modified DNA. This alteration did not much affect the scission efficiency. See the Supporting Information for details.
(17) The pK_a value of methyl 9-acridinecarboxylate is 3.2 (see ref 11).
(18) Kuzuya, A.; Machida, K.; Mizoguchi, R.; Komiyama, M. *Bioconj. Chem.* **2002**, *13*, 365−369.
(19) The fluorescence from 2-methoxy-6-chloro-9-aminoacridine is strongly quenched, when the acridine ring intercalates between the GC base pair: (a) Steiner, R. F.; Kubota, Y. In *Excited States of Biopolymers*; Steiner, R. F., Ed.; Plenum: New York, 1983; pp 203−254. (b) Hess, S.; Götz, M.; Davis, W. B.; Michel-Beyerle, M. E. *J. Am. Chem. Soc.* **2001**, *123*, 10046−10055.
(20) Specially designed dinuclear and trinuclear Zn(II) complexes are eminent for RNA hydrolysis: (a) Yashiro, M.; Ishikubo, A.; Komiyama, M. *J. Chem. Soc., Chem. Commun.* **1995**, 1793−1794. (b) Yashiro, M.; Ishikubo, A.; Komiyama, M. *J. Chem. Soc., Chem. Commun.* **1997**, 83−84. (c) Matsuda, S.; Ishikubo, A.; Kuzuya, A.; Yashiro, M.; Komiyama, M. *Angew. Chem., Int. Ed. Engl.* **1998**, *37*, 3284−3286.
(21) Shimayama, T.; Nishikawa, S.; Taira, K., *Biochemistry* **1995**, *34*, 3649−3654.
(22) Pérez-Ruiz, M.; Barroso-delJesus, A.; Berzal-Herranz, A. *J. Biol. Chem.* **1999**, *274*, 29376−29380.
(23) Warashina, M.; Kuwabara, T.; Nakamatsu, Y.; Taira, K. *Chem. Biol.* **1999**, *6*, 237−250.

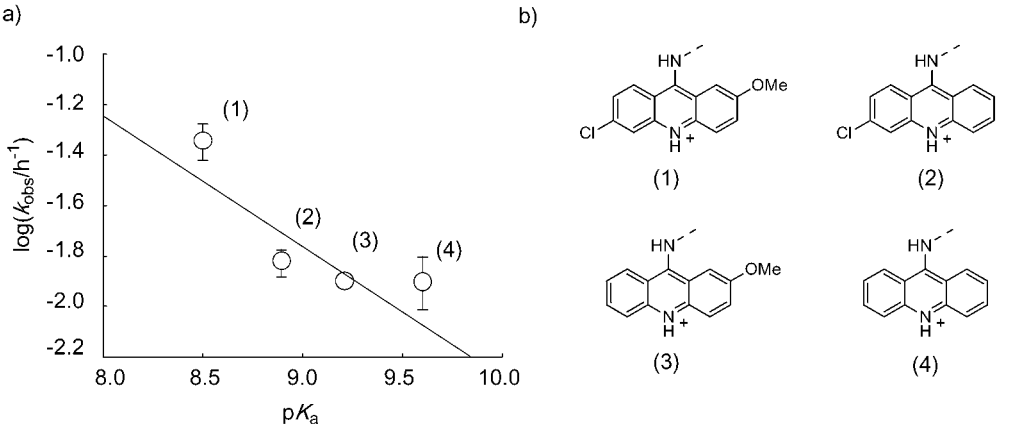

Figure 10. log−log plot of observed rate constant vs acidity of the acridine (a). Structures of the acridines are listed in part b. The pK_a value of each acridine is adopted from ref 11.

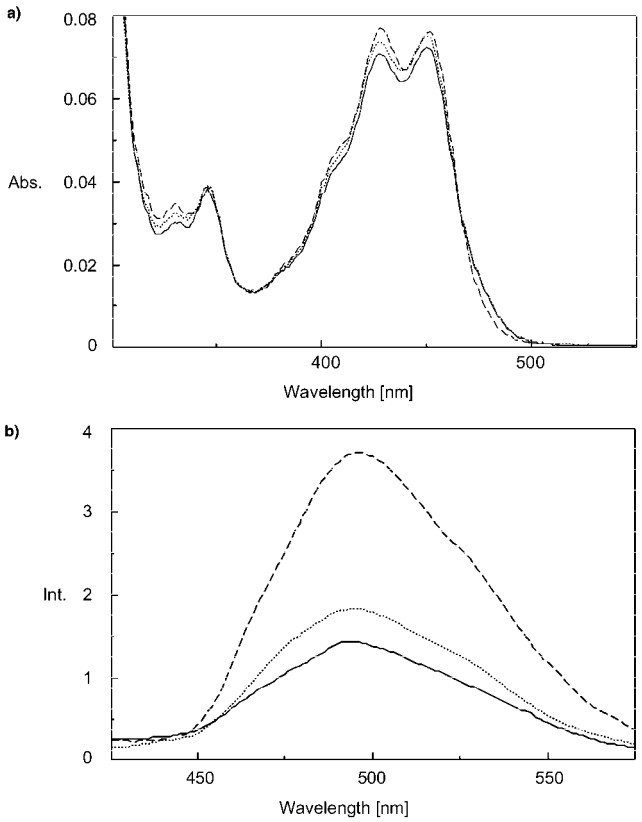

Figure 11. Absorption (a) and fluorescence (b) spectra of the acridine of DNA_{L1}-Acr at pH 8.0 and 37 °C. For both parts a and b, the solid line is for the DNA_{L1}-Acr/DNA_{R2}/RNA_1 system, the broken line is for DNA_{L1}-Acr alone, and the dotted line is for the DNA_{L1}-Acr/RNA_1 system; in 10 mM Tris-HCl containing 200 mM NaCl; [modified or unmodified DNAs] = [RNA_1] = 10 (a) and 2 μM (b).

is preferentially cleaved is dependent on the kind of metal ion. Heavy lanthanide ions (e.g., Lu(III) and Yb(III)) and the Zn(II) ion choose the 5′-side linkage, whereas light lanthanide ions (e.g., La(III) and Ce(III)), Mn(II), and Mg(II) prefer the 3′-side. The scissions at these two linkages proceed independently from each other, as experimentally evidenced. Apparently, there are two reaction sites for each of these scissions, and their contributions to RNA hydrolysis are governed by physicochemical properties of the metal ion (ionic radius, coordination manner, and others). Otherwise, all the metal ions would have shown similar 5′/3′ selectivities.[24]

Proposed Mechanism of Site-Selective RNA Activation. Spectroscopic analyses have shown that the acridine group is stacked between two adjacent DNA/RNA Watson−Crick base pairs in the heteroduplexes between the type-II activators and RNA (Figure 11). As the result of this exclusive intercalation of acridine,[25] the unpaired base opposite the acridine is flipped out from the duplexes between DNA and acridine-modified DNA. Accordingly, the conformation of the RNA backbone at the target site is changed and the positively charged acridine is placed near the scissile phosphodiester linkages. The site-selective RNA scission is primarily ascribed to the acid catalysis by the acridine residue, as is clearly indicated by the Brønsted plot in Figure 10. Thus, the protonation of the acridine is essential for the site-selective scission (9-acridinecarboxamide, which exists as neutral species, is virtually inactive for the present reaction: see the Results section). It is also possible that the conformation of the backbone at the target site is altered from the one that is more favorable for the intramolecular attack by 2′-OH. This factor further promotes the site-selective reaction. A similar conformational change is indicated in RNA scission by ribozymes.[26]

The proposed mechanism completely agrees with the following results obtained on the reactions with the type-II activators. (1) The second unmodified oligonucleotide (DNA_{R1} in the DNA_{L1}-Acr/DNA_{R1} combination) is essential for the efficient RNA activation (lanes 5 and 7 in Figure 8); "sandwiching" of the acridine by the neighboring Watson−Crick base pairs is significant. (2) When acridines are attached to both of the oligonucleotides and the "sandwiching" is hindered by steric repulsion, the RNA activation is minimized (lane 5 in Figure 7). (3) Unpaired ribonucleotide in front of the acridine is indispensable; the activation is virtually nil when an acridine group is incorporated into the completely complementary duplex (lane 2 in Figure 8). (4) Simple addition of acridine to the reaction mixture without any covalent attachment to oligonucleotides induces no RNA activation (data not presented).

Since the acridine group is located in the firmly structured DNA/RNA heteroduplex, activation of the target linkage predominantly occurs near the fixed acridine. In bulge-based

(24) When the 5′/3′ ratios are plotted against the ionic radius for all the metal ions investigated (including non-lanthanide ions), no fair relationship is obtained. Many other factors are also responsible here.
(25) Fukui, K.; Tanaka, K. *Nucleic Acids Res.* **1996**, *24*, 3962−3967.
(26) Murray, J. B.; Terwey, D. P.; Maloney, L.; Karpeisky, A.; Usman, N.; Beigelman, L.; Scott, W. G. *Cell* **1998**, *92*, 665−673.

strategies, however, the acid catalyst is absent, and furthermore the strain energy at the bulge is spread over several phosphodiester linkages and cannot much activate the target linkage. The possibility that the modified oligonucleotides simply provide unpaired ribonucleotide as the reactive site is concretely ruled out by the fact that DNA_{F1}-S never promotes the scission (lane 8 in Figure 2). To obtain the present prompt scission, the RNA must be activated by noncovalent interactions with the acridine.

Conclusion

Novel sequence-selective RNA cutters are synthesized by combining modified oligonucleotide(s) with catalysts for RNA hydrolysis. The target phosphodiester linkages are selectively activated by noncovalent interactions with the oligonucleotide, whereas the others are deactivated on the formation of the heteroduplex. Thus, the site-selective scission is successfully accomplished, although the catalysts are never bound to any sequence-recognizing moiety. The scissions require no specific sequence, and thus any target site is hydrolyzed in a desired specificity. When necessary, various chemical and physiological functions can be provided by appropriate chemical modification. Both the scission rates and selectivity can be further improved, leading to versatile applications for molecular biology, biotechnology, therapy, and others.

Experimental Section

Preparation of Oligonucleotides. Reagents were purchased from Glen Research Co. Automated syntheses of DNA and RNA were performed on an ABI 394 DNA synthesizer in 1 μmol scale. Deprotection of acridine-modified oligonucleotides and their removal from the support were achieved by 0.4 M methanolic sodium hydroxide in a 4:1 methanol−water mixture.[10] All other oligonucleotides were treated with concentrated aqueous ammonia. Crude oligonucleotides were purified by Poly-Pak II cartridges (Glen Research Co.), 20% denaturing PAGE, and then by a reversed-phase HPLC equipped with an RP-C18 column (Cica-Merck LiChroCART 125-4: a linear gradient of 5−25% acetonitrile in 0.05 M ammonium formate over 20 min; flow rate 0.5 mL/min). All the oligonucleotides were completely characterized by mass spectrometry (a KRATOS Kompact MALDI 2 TOF-MS spectrometer).

RNA Cleavage Assay. The substrate RNA (5′-end ^{32}P-labeled) and the corresponding complementary oligonucleotide bearing an acridine (1 and 10 μM final concentrations, respectively) were dissolved in 10 mM Tris-HCl buffer (pH 8.0) containing NaCl (200 mM). The mixture was heated to 90 °C (for 1 min), and slowly cooled to room temperature. Then 1/10 volume of aqueous solution of metal chloride (or nitrate) was added to the mixture. The metal salts were commercially obtained. After a predetermined reaction time at 37 °C in the dark, the reaction was quenched by 100 mM EDTA-2Na solution and analyzed on 20% denaturing PAGE. Imaging and quantification of RNA cleavage were carried out on a Fuji film FLA-3000G fluorescent imaging analyzer.

TOF-MS Analyses of the Cleavage Fragments. Fluorescein-labeled (at either the 3′ or the 5′ end) RNA substrates were cleaved by DNA_{F1}-Acr and Lu(III) under the conditions described above. After 24 h, the reaction was quenched by 100 mM EDTA-2Na solution and desalted with MicroSpin G-25 Columns (from Amersham Pharmacia Biotech). The fragments were purified by PAGE and HPLC, and then analyzed by MALDI TOF-MS (Supporting Information, Figure 5).

Spectroscopy. UV−vis spectra were obtained on a JASCO V-530 spectrometer at 37 °C in pH 8 Tris-HCl buffer (10 mM) containing modified or unmodified DNAs (10 μM), RNA_1 (10 μM), and NaCl (200 mM). Fluorescence spectra were measured on a JASCO FL-735 spectrometer with the excitation of the acridine at 346 nm. For CD spectroscopy, a JASCO J-725 spectropolarimeter was used.

Acknowledgment. This work was supported by the Bio-oriented Technology Research Advancement Institution. The support by a Grant-in-Aid for Scientific Research from the Ministry of Education, Science, Sport, and Culture, Japan is also acknowledged.

Supporting Information Available: A table of scission efficiencies with various target sequence; figures of site-selective RNA scission by Zn(II), Mg(II), Cu(II), Ni(II), and Co(II); results of the scission of 2′-*O*-methyl-introduced substrates; TOF-MS spectra of fragments; structures, syntheses, and characterizations of acridine-modified DNA in Figure 10b (PDF). This material is available free of charge via the Internet at http://pubs.acs.org.

JA025653P